

**Biochemical and Structural Characterization of Germicidin Synthase: Analysis of a Type III  
Polyketide Synthase that Employs Acyl-ACP as a Starter Unit Donor**

Joseph A. Chemler, Tonia J. Buchholz, Todd W. Geders, David L. Akey, Christopher M. Rath, George E.  
Chlipala, Janet L. Smith, and David H. Sherman\*

\* Life Sciences Institute, Departments of Chemistry, Medicinal Chemistry, and Microbiology &  
Immunology, University of Michigan, Ann Arbor, MI 48109

Supporting Information

## **Table of Contents**

### **Methods**

LC-MS of enzymatic reactions.	S3
Characterization of enzymatically-synthesized germicidin A.	S3

### **Supporting Figures**

Figure S1. Sequence comparisons among selected type III PKSs.	S3
Figure S2. Size exclusion chromatography of Gcs.	S6
Figure S3. LC-MS of germicidin A produced by type II fatty acid synthase and Gcs.	S7
Figure S4. LC-MS Analysis of formation of 3-oxo-4-methyl-pethyl-CoA by FabH.	S9
Figure S5. Kinetics curves of Gcs.	S10
Figure S6: Gcs binding specificity towards AcpP Is not significantly affected by mutations to arginine surface residues.	S11

### **Supporting Tables**

Table S1. Primers used for mutagenesis of Gcs.	S12
--	-----

## Methods

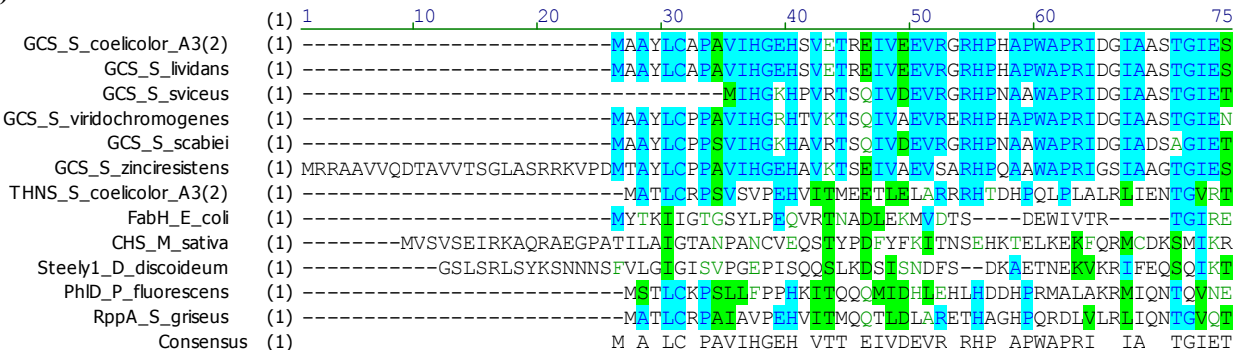
**LC-MS of enzymatic reactions.** LC-MS analysis was performed with a Shimadzu LCMS-2010EV mass spectrometer (Columbia, MD) with an Agilent Zorbax Stablebond C18 reverse phase column (4.6 x 150 mm). 10  $\mu$ l samples were separated under isocratic conditions of 25% CH<sub>3</sub>CN (vol/vol) with 0.1% (vol/vol) formic acid over 20 min at a flow rate of 0.5 mL/min at room temperature. Samples were desalted online by diverting the flow to waste for five min before switching the divert valve to the MS detector. The absorbance at 290 nm was monitored and profile mode data was gathered from m/z 100-300 utilizing electrospray ionization in scanning ion mode.

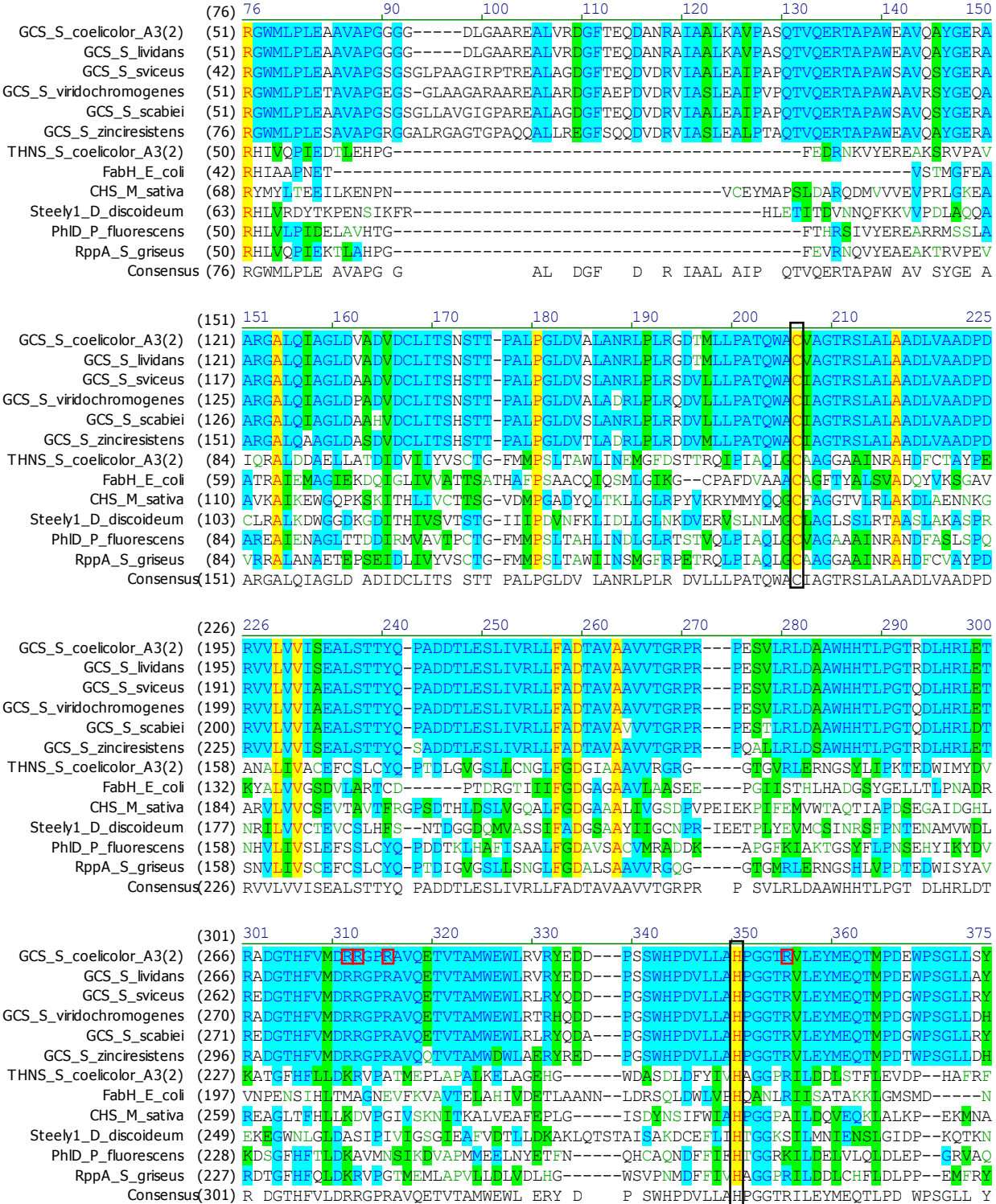
**Characterization of enzymatically-synthesized germicidin A.** The NMR data were recorded at 600 MHz for <sup>1</sup>H on a Varian Performa IV spectrometer with a Protasis CapNMR inverse dual-band probe. Proton chemical shifts are reported relative to the residual proton signal of the deuterated solvent MeOH-*d*<sub>4</sub> (3.29 ppm).

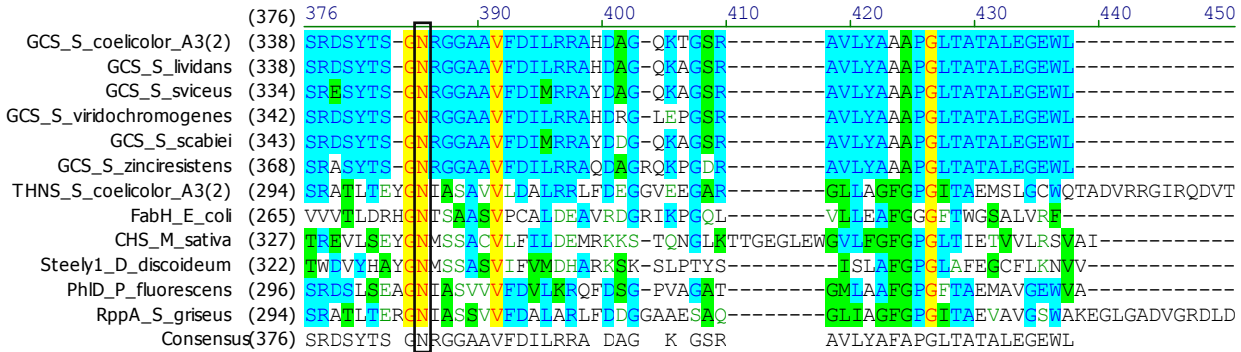
Germicidin A: <sup>1</sup>H NMR (600 MHz, MeOH-*d*<sub>4</sub>)  $\delta$  1.01 (t, *J*=7.4 Hz, 3H), 1.20 (d, *J*=7.0 Hz, 6H), 2.37 (q, *J*=7.4 Hz, 2H), 2.68 (spt, *J*=7.0 Hz, 1H), 5.91 (s, 1H).

UV:  $\lambda_{\text{max}}$  (202, 290 nm). Low resolution ESI-MS: [M+H]<sup>+</sup> = 183.00 m/z; expected = 183.10.

a)







b)

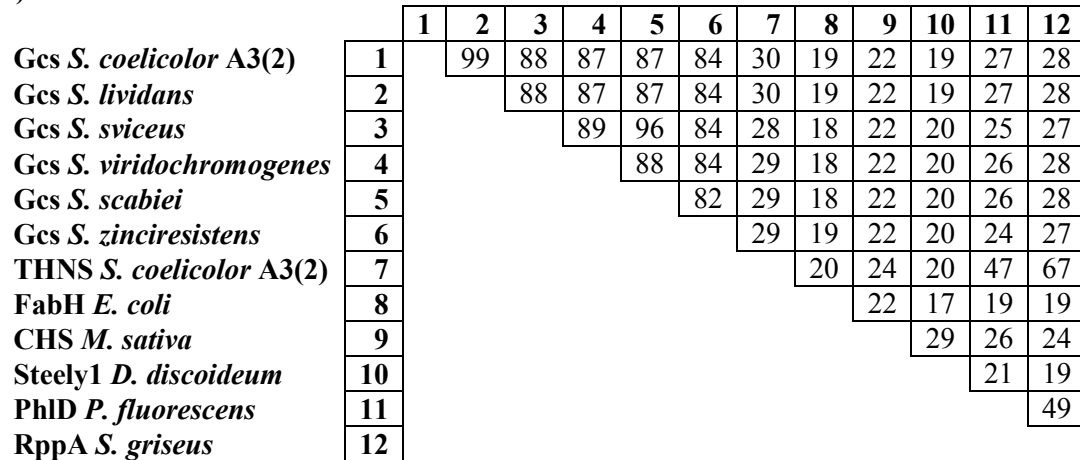


**Figure S1.** Sequence comparisons among selected type III PKSs. a) Sequence alignments for Gcs and selected proteins. Catalytic triad residues are boxed in black. Gcs arginine residues selected for mutation are boxed in red. b) Percent sequence identities of aligned type III PKSs and FabH proteins.

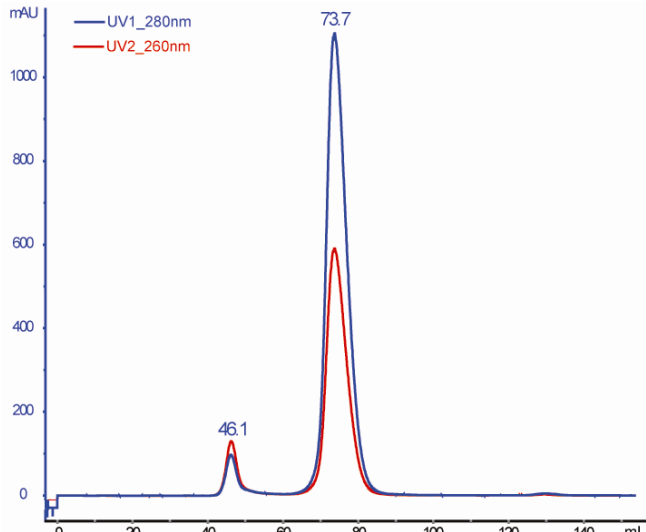


**Figure S2.** Size exclusion chromatography of Gcs. Mobile phase consisted of 20 mM HEPES, pH 7.4, 150 mM NaCl, 10% glycerol, 0.5 mM TCEP. The peak around 45 mLs represents material eluting near the void volume. The major protein peak eluted at 74 mLs. To calculate the apparent molecular weight, this elution volume was fit to the equation,  $mLs = -12.447 * \ln(MW) + 129.52$  (MW in kDaltons). An apparent molecular weight of 90,000 Daltons is consistent with a dimer for the His-tagged protein whose calculated molecular weight is 44,000 Daltons.

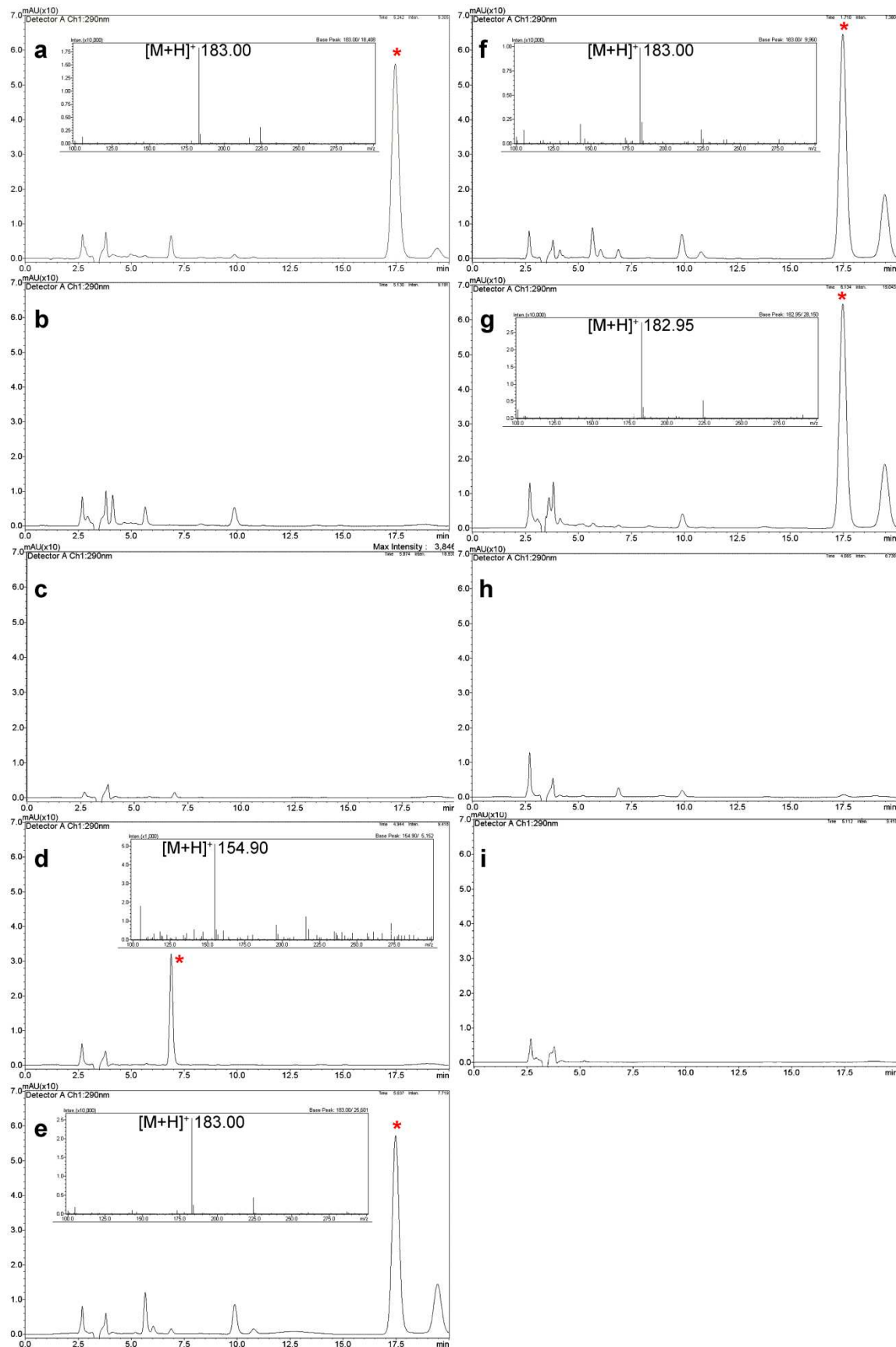


**Figure S3.** LC-MS of germicidin A produced by type II fatty acid synthase and Gcs. All LC traces were analyzed at 260 nm. All reaction consists of all or minus one of the following components: apo/holo-AcpP, AcpS, FabD, FabH and Gcs along with free CoA, malonyl-CoA, isobutyryl-CoA and ethylmalonyl-CoA. a) Reaction consisting of all components. The insert is the positive ESI mass spectrum of the major peak (germicidin A) labeled with a red asterisk. b) Reaction without malonyl-CoA. c) Reaction without ethylmalonyl-CoA. d) Reaction without isobutyryl-CoA. e) Reaction without AcpP. f) Reaction without AcpS. g) Reaction without FabD. h) Reaction without FabH. i) Reaction without Gcs.

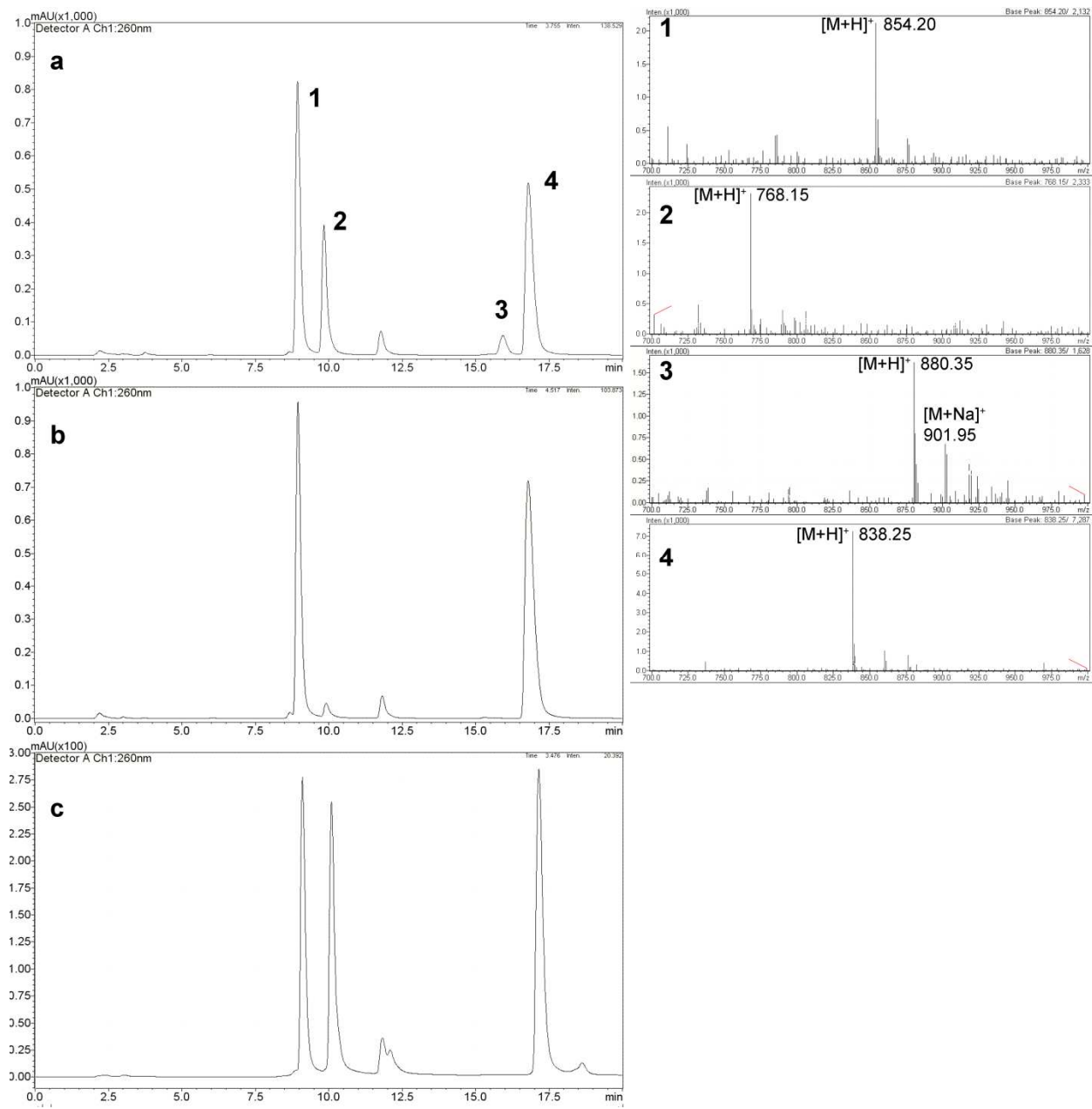


**Figure S4.** LC-MS analysis of formation of 3-oxo-4-methyl-pentyl-CoA by FabH. All traces were analyzed at 260 nm. a) FabH reaction using malonyl-CoA (1) and isobutyryl-CoA (4) to form free CoA (2) and 3-oxo-4-methyl-pentyl-CoA (3). The right panel shows the positive ESI mass spectrum of peaks. b) Control reaction without FabH. c) CoA standards of malonyl-CoA, free CoA, and isobutyryl-CoA.

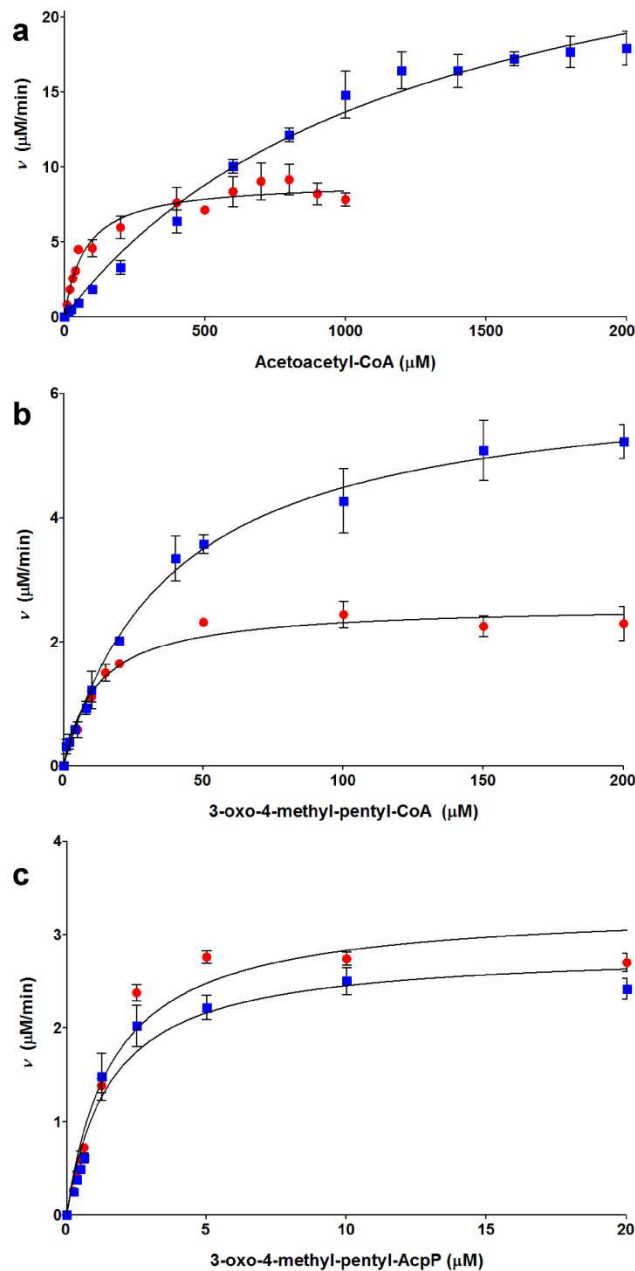


**Figure S5.** Kinetics curves of Gcs. Rate of formation of pyrone product from reactions containing a) acetoacetyl-CoA b) 3-oxo-4-methyl-pentyl-CoA and c) 3-oxo-4-methyl-pentyl-AcpP. Reactions with acetoacetyl-CoA proceeded with 3  $\mu\text{M}$  Gcs for five minutes while all other reactions proceeded with 0.3  $\mu\text{M}$  Gcs for one minute. Red circles indicate reactions contained 1 mM methylmalonyl-CoA and blue squares indicate reactions contained 1 mM ethylmalonyl-CoA.

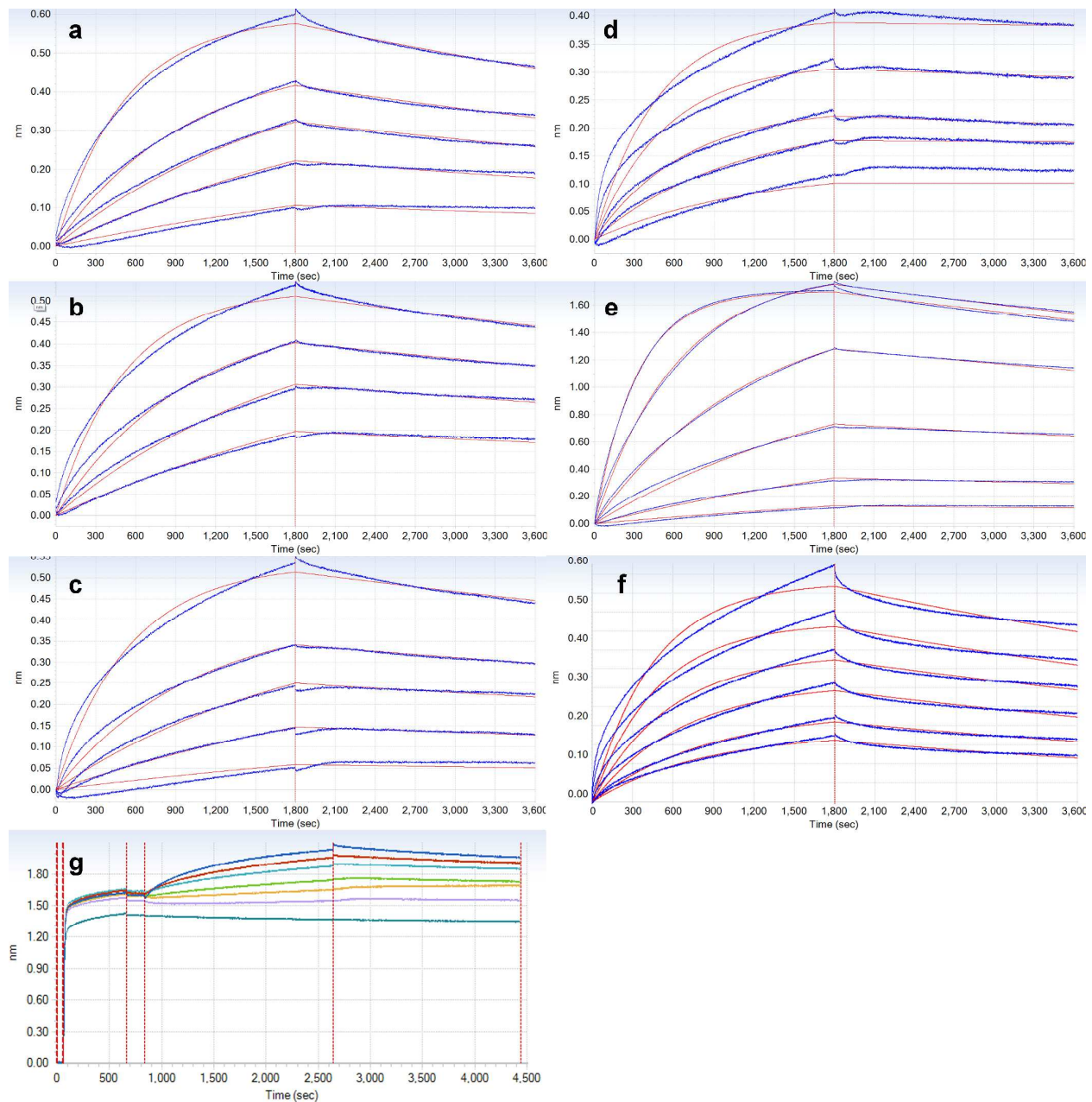


**Figure S6:** Gcs binding specificity towards AcpP Is not significantly affected by mutations to arginine surface residues. Biolayer interferometry measurements of Gcs and mutants binding directly to biotinylated AcpP immobilized onto streptavidin sensors. a) Gcs wild type, b) R276A, c) R277A, d) R280A, e) R317A, and f) R276/317A. Shift data, aligned to the start of the association step, are shown in blue and fitted binding curves are in red. g) Example of the raw data including immobilization of biotinylated-AcpP onto the streptavidin biosensors followed by equilibration to a baseline in 1X PBS buffer before association and dissociation of with Gcs wild-type.

**Table S1.** Primers used for mutagenesis of Gcs.

Primer name	Primer sequence	Constructed plasmid
R276A_F	ttcgtgatggacgctcgccggccgcg	pDHS9753
R276A_R	cgcggcccgcgagcgcatcacgaa	
R277A_F	tgatggaccggccggccgcgg	pDHS9807
R277A_R	cccgccggccggccggcatca	
R280A_F	gcggggccggggggcggtgcag	pDHS9790
R280A_R	ctgcaccgcggccggccgcgc	
R317A_F	cccgccggaccgcgggtgtggagta	pDHS9791
R317A_R	tactccagcaccgcggteccgcggg	
pET_F	ctcgatcccgcgaaattt	
pET_R	ccggatatagttccctttc	
Δ63-96_R	ggacggctgtcgacgcggcgcgacggccgcctccaggggagca	pDHS9794
Δ63-96_F	cctggaggccgcgtcgccccgcgtcgacaccgtccaggagcgc	
Δ63-97_R	cctggacggctgtcgacgcgcgcgacggccgcctccaggggagca	pDHS9795
Δ63-97_F	cctggaggccgcgtcgccgcgtcgacaccgtccaggagcgcacc	
Δ63-98_R	tcctggacggctgtcgacgcgcggccctccaggggagca	pDHS9793
Δ63-98_F	tggaggccgcgtcgacaccgtccaggagcgcaccgc	

## References

- (59) Concepcion, J., Witte, K., Wartchow, C., Choo, S., Yao, D., Persson, H., Wei, J., Li, P., Heidecker, B., Ma, W., Varma, R., Zhao, L.S., Perillat, D., Carricato, G., Recknor, M., Du, K., Ho, H., Ellis, T., Gamez, J., Howes, M., Phi-Wilson, J., Lockard, S., Zuk, R., Tan, H. *Comb. Chem. High Throughput Screening* **2009**, *12*, 791.